

Tools for quantifying N₂O emissions from agroecosystems

E. Pattey ^{a,*}, G.C. Edwards ^a, R.L. Desjardins ^a, D.J. Pennock ^b, W. Smith ^a,
B. Grant ^a, J.I. MacPherson ¹

^a Environmental Health, Agriculture and Agri-Food Canada, 960 Carling Avenue, Ottawa, Ont., Canada K1A 0C6

^b University of Saskatchewan, Department of Soil Science, 51 Campus Drive, Saskatoon, Sask., Canada S7N 5A8

Received 16 May 2005; received in revised form 17 May 2006; accepted 22 May 2006

Abstract

The importance of constraining the global budget of nitrous oxide (N₂O) has been well established. The current global estimate of the contribution of N₂O to total anthropogenic greenhouse gas emissions from agriculture is about 69%. Considerable progress has been made over the past few years in developing tools for quantifying the emissions from agricultural sources, at the local and field scale (i.e., chamber and tower-based measurements) as well as at the landscape and regional levels (i.e., aircraft-based measurement and modelling). However, aggregating these emissions over space and time remains a challenge because of the high degree of temporal and spatial variability. Emissions of N₂O in temperate climate are largely event driven, e.g., in Eastern Canada, large emissions are observed right after snowmelt. The average emissions during the snowmelt period vary considerably, reflecting the influence of many controlling factors. Cumulative emissions reported here range from 0.05 kg N₂O-N ha⁻¹ in Western Canada to 1.26 kg N₂O-N ha⁻¹ in Eastern Canada, values that reflect differences in climatic zones and fertilizer management practices. This paper describes the tools for refining the global N₂O budget and provides examples of measurements at various scales. Tower-based and aircraft measurement platforms provide good data for quantifying the variability associated with the measurements. Chamber-based methods lack the temporal and spatial resolution required to follow the event driven nature of N₂O fluxes but provide valuable information for evaluating management practices. The model DeNitrification and DeComposition is an example of a technique to estimate N₂O emissions when no data is available.

Crown Copyright © 2006 Published by Elsevier B.V. All rights reserved.

Keywords: Flux measurement tools; Modelling; Snowmelt N₂O release

1. Introduction

A major proportion of the contribution from agriculture to greenhouse gas emissions comes from N₂O. In 1990, emissions from agriculture were estimated to be 2.5 Tg N₂O year⁻¹, i.e., 67% of the anthropogenic N₂O emissions reported from countries

included in Annex I to the Framework Convention on Climate Change (UNFCCC, 2003). Ten years later, slightly lower agricultural emissions, 2.2 Tg N₂O year⁻¹, still represented 69% of the global anthropogenic N₂O emissions. In 1990, the top 10 countries contributing most to agricultural N₂O emissions were USA (901 Gg year⁻¹), Russian Federation (280 Gg year⁻¹), France, Germany, UK, Canada (100–192 Gg year⁻¹) Japan, Italy, Australia and Spain (59–76 Gg year⁻¹). Between 1990 and 2000, a significant increase was reported for USA, Canada, Australia and Spain, while emissions were relatively steady for Italy and a reduction was reported for Russian Federation

* Corresponding author. Fax: +1 613 759 1724.

E-mail address: pattey@agr.gc.ca (E. Pattey).

¹ Formerly with Flight Laboratory of National Research Council, Ottawa, Ont., Canada.

(until 1999), Japan, France, Germany and UK. The main sources of N₂O are agricultural soils, manure management and residue burning. Emissions from agricultural fields are mostly associated with denitrification following fertilizer application when soil moisture reaches field capacity, and to a lesser extent with nitrification (Bouwman, 1990). In the USA, N₂O emissions from agriculture are mainly associated with field crop production (94.4%), manure management (5.4%) and crop residue burning (0.1%) (EPA, 2001). Other countries show similar sources; however, the total emissions change drastically for countries using limited amounts of synthetic fertilizers. Recent recalculations to improve the quality of estimates of national inventory reports showed that N₂O had the largest changes between the new national estimates and the previous ones, with differences ranging from -23 to 178%, compared to CH₄ and CO₂ national estimates which were relatively steady (UNFCCC, 2004). Measuring N₂O emissions is still a challenge, which makes the inventories of emissions complex to establish. Indeed, emissions are highly variable in time and space, therefore despite the many efforts to refine estimates, the uncertainty surrounding the agricultural emissions is still high (Grant and Pattey, 2003; Desjardins, 2004).

Nitrous oxide emissions in temperate climate are largely event driven, with rainfall being a critical factor. Moreover, in cold climate, the spring thaw period has been shown to result in large emissions (Goodroad and Keeney, 1984; Cates and Keeney, 1987; Wagner-Riddle et al., 1997; Wagner-Riddle and Thurtell, 1998; Grant and Pattey, 1999; Corre et al., 1999; Van Bochove et al., 2000; Pennock and Corre, 2001), and is estimated to contribute about 30–50% of yearly emissions from fertilized fields (Smith et al., 2004). The thaw period provides ideal conditions for the release of N₂O produced during the winter through denitrification both below and in the frozen soil layer (Teepe et al., 2001). These emissions are mostly associated with the development of anoxic conditions in the soil induced by precipitation and snowmelt water. However, the numerous factors influencing the emissions (Dörsch et al., 2004) cannot all be quantified on time and space scales needed to fully understand the processes responsible for large emissions after snowmelt. Consequently, this has hindered progress on the development of models that describe adequately the spring thaw emission phenomenon.

In order to improve emission estimates, a multiscale approach using a combination of measurements and models is required. This paper presents various tools that are available for measuring and estimating N₂O

emissions from agricultural diffuse sources and examines results obtained using chamber-, tower-, and aircraft-based flux measurements as well as the use of process-based models for integrating the emissions over space and time for two case studies carried out in Canada during the spring thaw period.

2. Tools for quantifying N₂O emissions at field, landscape and regional scales

Chamber, tower and aircraft platforms are available for quantifying N₂O emissions from agricultural fields. Chambers are the most widespread as they rely on widely available gas chromatography for determining N₂O concentration. Tower and aircraft platforms, which have been extensively used for measuring CO₂/H₂O fluxes, can be used to measure N₂O fluxes due to the development of the tunable diode laser technology. All methods are needed in addition to process-based modelling to quantify emissions at the field, landscape and regional scales.

2.1. Chamber-based N₂O flux measurement

Chambers have been used extensively for the quantification of N₂O emissions from agroecosystems (Livingston and Hutchinson, 1995; Mosier et al., 1994; Rochette and McGinn, 2004). They are very useful for quantifying the impact of various treatments but their coverage is limited over space and time. They are also intrusive and tend to modify the environmental conditions during the measurement. Their use is labour intensive because, in the case of N₂O, measurements are difficult to automate. The most suitable chamber type is the non-steady-state and non-flow-through chamber (Livingston and Hutchinson, 1995). During the deployment of this type of chamber, N₂O emitted from soil surface is accumulating. The flux (F_{N_2O} , mol N₂O m⁻² s⁻¹) is proportional to the rate of concentration change in the chamber head space over time ($\partial[N_2O]/\partial t$, mol N₂O mol⁻¹ dry air s⁻¹):

$$F_{N_2O} = \left(\frac{\partial[N_2O]}{\partial t} \right) \left(\frac{V_h}{A} \right) \left(\frac{1 - e/P}{V_M} \right) \quad (1)$$

where t is the time (s), $\partial[N_2O]/\partial t$ is determined on dry air samples and estimated at the initial time of deployment, V_h (m³) is the headspace volume of the chamber, A is the chamber area (m²), V_M (m³ mol⁻¹) is the mole volume using chamber air temperature at the initial time of deployment, e (kPa) is the water vapor pressure inside the chamber at the initial time of deployment

and P (kPa) is the atmospheric pressure. The strengths and weaknesses of chamber techniques as well as methodological precautions and QC/QA were reviewed by [Rochette and McGinn \(2004\)](#). They recommend optimizing the duration of chamber deployment for minimizing the inherent bias when determining the N_2O initial slope, extracting at least three to four head space air samples for characterizing the non-linearity in the change of concentration over time, and taking extra care to avoid leakages during the deployment of the chambers.

2.2. Tower-based N_2O flux measurement

Tower-based micrometeorological flux measurements permit non-intrusive quantification of trace gas exchange over time. They integrate fluxes over larger space (i.e., field scale) and provide almost continuous time series (interruption under low wind velocities and for either instrument maintenance or failure). Tower-based flux measurements also permit for the experimental measurement of controlling factors. The resulting data can therefore be used to verify the performance of process-based models for estimating the flux at the field scale. As they require high initial investment and expertise, they cannot be used in factorial designs, based on repetitions, as chambers can be.

The tower-based N_2O flux measuring system routinely used in Canada is based on a close-path single-pass tunable diode laser (TDL) (TGA100, Campbell Scientific Inc., Logan, UT). It is designed to make measurement of the mole fraction in differential mode, by continuously calculating the absorbance ratio of ambient air samples over a reference gas ([Edwards et al., 2003](#)). It does not require any specific calibration and is insensitive to pressure and temperature fluctuations in the air sampling stream; however, it requires accurate knowledge of the reference gas concentration ([Pattey et al., 2006a](#)). Other custom-made TDL based trace gas analyzers are available (e.g., TDL-36, Aerodyne Research, Billerica, MA, USA), and have been used by several research teams in Europe and USA ([Weinhold et al., 1994; Zahniser et al., 1995; Laville et al., 1999](#)). The TGA100 has been used extensively to measure trace gas concentration gradients in order to determine the flux using the flux-gradient technique ([Edwards et al., 1994, 2001, 2003; Wagner-Riddle et al., 1996a,b; Wagner-Riddle and Thurtell, 1998; Simpson et al., 1995, 1997; Grant and Pattey, 1999, 2003](#)). The flux-gradient technique is chosen over the more direct eddy covariance method as it permits the use of one

TGA100 to measure fluxes over several locations sequentially.

2.2.1. Flux-gradient technique

The average vertical N_2O flux, based on the flux gradient approach, is calculated as follows:

$$F_{\text{N}_2\text{O}} = \frac{-u_* k (\rho_{\text{N}_2\text{O}_2} - \rho_{\text{N}_2\text{O}_1})}{[\ln((z_2 - d)/(z_1 - d)) - \psi_{h_2} + \psi_{h_1}]} \quad (2)$$

where by convention, a positive flux is upwards, u_* is the friction velocity (m s^{-1}), k is the von Karman constant (0.4), z_1 and z_2 are the lower and upper sample air intake heights (m), respectively, $\rho_{\text{N}_2\text{O}_1}$ and $\rho_{\text{N}_2\text{O}_2}$ are the N_2O concentrations at z_1 and z_2 , respectively, d is the zero-plane displacement height (m) and ψ_{h_1} and ψ_{h_2} are the integrated similarity functions for heat at z_1 and z_2 . Note the eddy diffusivity $K(z)$ ($\text{m}^2 \text{s}^{-1}$), where $K(z) = u_* k (z_2 - z_1) / [\ln((z_2 - d)/(z_1 - d)) - \psi_{h_2} + \psi_{h_1}]$ is implicit in the equation. The integrated similarity functions are stability dependent ([Hicks, 1976; Paulson, 1970](#)) and require the calculation of the Monin–Obukhov length, L (m). A 3D ultrasonic anemometer is used to measure supporting variables such as momentum, and sensible and latent heat fluxes by the eddy covariance technique to compute L and u_* .

For measuring the flux, a Nafion dryer (PD-1000-48SS, Perma Pure, Tom River, NJ) is used to completely remove water vapor from the air collected. The TDL flux gradient system is designed so that the air collected has time to equilibrate with the TDL temperature. These features eliminate the need for the correction of density fluctuations in the flux calculations ([Webb et al., 1980](#)).

2.2.2. Eddy covariance technique

The eddy covariance method is the most direct method for measuring the flux over a surface. The method involves the simultaneous measurement of wind velocities and scalar mixing ratios of interest. The trace gas flux is expressed as follows:

$$F_S = \bar{\rho}_a \left(\frac{M_s}{M_a} \right) \overline{w' s'} \quad (3)$$

where ρ_a is the density of dry air (g m^{-3}), M_s and M_a are the molecular masses of the scalar and of dry air (g mol^{-1}), w is the vertical velocity (m s^{-1}), and s is the molar mixing ratio of the scalar (nmol mol^{-1} dry air), primes denote the fluctuations and the overbar represents a time average. A more thorough description of the eddy covariance method as applied to these measurements is given in [Pattey et al. \(2006a\)](#).

2.3. Aircraft-based N_2O measurement

Aircraft-based fluxes have been obtained for the last two decades for gases such as CO_2 and H_2O (Desjardins et al., 2000). This is an excellent platform for obtaining flux measurements at the regional scale, i.e., 10–100 km. However, it provides flux measurements for short periods of time only, which can be repeated from day-to-day. It is relatively expensive. The National Research Council (NRC) and AAFC have collaborated during the last few years to develop an instrumented aircraft platform for the measurements of trace gas fluxes (e.g., Zhu et al., 1999). The NRC Twin Otter aircraft is instrumented to measure the three components of atmospheric turbulence over a frequency range 0–16 Hz, as well as turbulent fluxes of momentum, sensible and latent heat, CO_2 and O_3 using the EC technique. Instrumentation and flux calculation procedures are described in detail in MacPherson et al. (2001). With a 10-Hz sampling rate, the aircraft platform has a spatial resolution on about 5.5 m, based on an averaged air-speed of 55 m s^{-1} .

The N_2O flux is measured using the relaxed eddy accumulation (REA) technique. Air samples are collected in PTFE bags. In order to prevent hysteresis/memory effects, these bags need to be flushed with ambient air then evacuated several times, prior to being used. Samples associated with upward and downward moving air are later analyzed in the laboratory using a TDL. A schematic of the REA aircraft sampling apparatus is shown in Fig. 1. Details of the laboratory setup for analyzing the air samples collected according to the vertical wind direction using the TGA100 are given in Pattey et al. (2006b).

The REA technique was first described in detail by Businger and Oncley (1990) and its application to aircraft platform by MacPherson and Desjardins (1991). The flux (F_{N_2O} , $\text{ng m}^{-2} \text{ s}^{-1}$) is expressed as follows:

$$F_{N_2O} = A\sigma_w (\overline{\rho_{N_2O}^+} - \overline{\rho_{N_2O}^-}) \quad (4)$$

where A is an empirical coefficient, which is about 0.56; σ_w is the standard deviation of the vertical wind velocity (m s^{-1}), ρ_{N_2O} is the N_2O density (ng m^{-3}), '+' indicates upward moving air and '-' indicates downward moving air. From run to run, the value of the coefficient A is estimated using the fast-response sensor signals from a scalar by simulating the conditional sampling of the REA technique (Pattey et al., 1993).

In the airborne REA sampling system for measuring inert gas, the air is drawn through a common 3/8 in. PTFE inlet, then pulled through two diaphragm pumps (NO23ANI, KNF Neuberger, Inc., Trenton, NJ), and split between the intakes collecting upward and downward moving air. After passing through 2-μm stainless steel filters (SS-6F-2, Swagelock), the air flow is maintained at a constant 12 L min^{-1} in each line by a mass-flow controller (MKS 1179A, MKS Instruments, Andover, MA) and a 4-channel power supply/readout unit (MKS 247C, MKS Instruments, Andover, MA). A relief valve (Swagelock) is used between each pump and each mass-flow controller to prevent over-pressure. Two fast-response switching 3-way valves (Honeywell-Skinner Valves, New Britain, CT) allow the air to either be collected in PTFE bags or vented in the plane. The vertical wind velocity signal controlling the switching of the valves is high-pass filtered in real time to remove

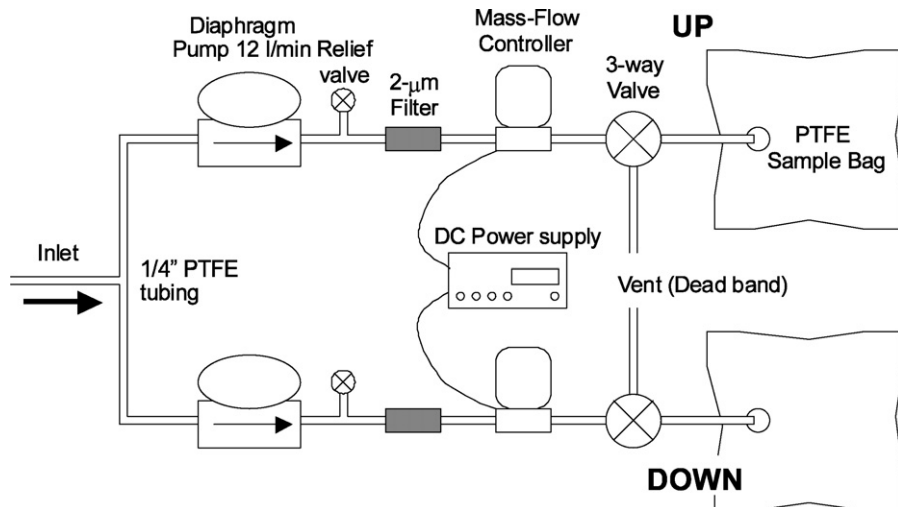


Fig. 1. Aircraft-based relaxed eddy accumulator using PTFE sampling bags as reservoirs.

any bias in sampling caused by low frequency eddies. This setup allows the use of a dead band, i.e., a range of w for which no air was collected.

2.4. Modelling

The sporadic nature of N_2O emissions requires the use of models for upscaling over time and space. Ecosystem modelling approach is used to predict emissions from soils. Models range from simple empirical to relatively complex process-based models. The IPCC (1997) empirical approach estimates emissions from fertilizer and manure as a fraction of their N content. This approach does not account for the effect of different management practices and climate.

Process-based models account for chemical, biological, and physical processes that contribute to the production of N_2O (Li et al., 1992a,b; Potter et al., 1996; Grant and Pattey, 1999; Parton et al., 1996); however, input data are often limited.

DeNitrification and DeComposition model (DNDC) (Li et al., 1992a,b) and DayCENT (Parton et al., 2001) are frequently used in the upscaling of greenhouse gas emissions from agricultural soils in Canada. These models are chosen because they require input variables that are relatively easy to obtain, the simulation time is short and, in the case of DNDC it has been calibrated for Canadian conditions (Smith et al., 2002, 2004; Grant et al., 2004). Only DNDC model was applied for comparison to the snowmelt data presented, since it has a module for the spring thaw.

The DNDC model (Li et al., 1992a,b, 1994; Li and Aber, 2000) consists of four interacting submodels that simulate daily and annual emissions from agricultural soils. Modelling emissions in Canada can be especially challenging due to the widespread climatic regimes across the country. Nitrous oxide emissions in temperate climates associated with spring thaw events can contribute up to 50% of the total emissions for any given year (Teepe et al., 2000; Kaiser et al., 1998). Recognizing this, the DNDC model has been upgraded to incorporate processes that deal with N_2O production from freezing and thawing events (Li and Aber, 2000). The four main assumptions, for a soil temperature below 0 °C, are as follows: (1) a constant fraction of the soil microorganisms will die and be added to the labile humads pool, (2) the oxygen diffusion rate will decrease due to the frozen surface, (3) the NO and N_2O produced will be confined in the soil until thawing occurs and (4) the thawing water flux will be the equivalent to a rainfall event to affect the soils biogeochemical processes based

on the model's routines. DNDC version 83P was used in this study.

2.5. N_2O emissions associated with snowmelt (Eastern Canada)

Tower-based flux measurements were obtained in 1997 from a Dalhousie clay loam field located southwest of Ottawa, Ontario (45°18'N and 75°44'W) between Calendar Day (CD) 57 and 71 when the snow cover was present and during the entire snowmelt and soil thawing period (CD 95–139). The field crops were barley (*Hordeum sativa* L.) in 1995 and corn (*Zea mays* L.) in 1996. The 23 ha field is relatively flat (slope <1%). The pH was 6.6 in the top 0.15 m, and the soil organic carbon content was 6.3%.

Thirty-minute average weather data and soil temperature profiles (0.05, 0.10, 0.20, 0.40, and 0.60 m depth) were collected during snowmelt. The site was equipped with a flux-gradient tower for measuring 30-min vertical gradients of N_2O at 1 and 2 m above the ground. The air sampled was dried close to the intake and brought to the TDL sampling cell under vacuum to perform sequential measurements through the two vertical levels using a switching frequency of 10 s. More details on the operation and setup of the TGA100 are provided in Edwards et al. (2003) and Pattey et al. (2006a). The 30-min flux standard error over a smooth surface ($z_0 \approx 0.01$ m) with $u_* = 0.2 \text{ m s}^{-1}$ and measurement intakes at 2 and 1 m was estimated to be 0.29 mg $N_2O\text{-N m}^{-2} \text{ d}^{-1}$ (Pattey et al., 2006a).

The eddy-flux tower, installed close to the N_2O -gradient system, was equipped with a 3D ultrasonic anemometer (10-cm open-path DAT-310, Kaijo-Denki, Tokyo, Japan) and a closed-path infrared $\text{CO}_2\text{-H}_2\text{O}$ analyzer (LI-6262, LI-COR, Lincoln, NE, USA) for measuring momentum flux, sensible and latent heat flux as well as CO_2 flux at 1.75 m above the surface. At this measuring height, the estimated footprint for integrating 80% of the cumulative flux extends between 200 and 400 m for u_* varying between 0.4 and 0.2 m s^{-1} under neutral conditions (Gash, 1986).

The TGA100 readings can be affected by several factors among which pressure fluctuations in the sampled air flow. During refilling of the Dewar, that hosts the diode laser, bubbling of the liquid nitrogen can affect the reading. Furthermore, the TGA100 is sensitive to vibration. The standard deviation of all the trace gas gradient data in a given half hour, which is proportional to the amplitude of the gradient, was used as a screening criterion of the 30-min N_2O gradient measurements of the TGA100. Once converted in

coefficient of variation, a criterion for screening large values can be established for detecting the impact of the refilling operation on the gradient and of other perturbations such as vibrations which may affect the laser beam, etc. Nighttime data were screened according to the two following conditions (Pattey et al., 2002): (1) a threshold criterion on u_* (i.e., 30-min gradient measurements were kept when $u_* > 0.06 \text{ m s}^{-1}$) and (2) that more than half of the nighttime 30-min gradient data met the u_* criterion. In this case, the daily flux integrates daytime and nighttime flux averages, otherwise the daily flux integrates the daytime flux average only. The latter case might lead to an overestimation of the daily flux, although an analysis showed that no significant relationship between N_2O flux and soil temperature at 0.05 or 0.10 m could be established.

2.6. N_2O emissions associated with snowmelt (Western Canada)

Aircraft and chamber flux measurements were collected 100 km north of Saskatoon, Saskatchewan in an agricultural area, close to Laird ($52^{\circ}43'\text{N}$ and $106^{\circ}30'\text{W}$). Detailed site description and methods were presented in Pennock et al. (2005). The region was selected because it offered a very homogeneous agroecosystem with crop types as the main variant. The experimental site was divided into 36 sections, each of which had four quarter sections of $800 \text{ m} \times 800 \text{ m}$. Twelve quarter sections were sampled for soil properties and used for measuring emission with the chambers. They included four quarters with pulse crop residues, four with small grain residues, and four with canola (*Brassica napus* L.) residues. Measurements were made for 7 days (i.e., 92–109) during the snowmelt period. Sampling was carried out during daytime hours (11:00–13:30 h). Ten samples were obtained for each site. One of the small grain quarters (NW2) received manure additions from the adjacent livestock operation. Nitrogen fertilizer (as urea or anhydrous ammonia) had been added at rates between 60 and 85 kg N ha^{-1} to all the canola and small grain sites except for NW2 in spring 2001. The pulse crop sites received a low rate of N ($\sim 10 \text{ kg N ha}^{-1}$) at the time of seeding.

The vertical flux density ($\text{mg N}_2\text{O-N m}^{-2} \text{ d}^{-1}$) above the soil surface was determined by measuring the change in gas concentration beneath the sealed chamber at equally spaced time intervals. The samples were analyzed using a Varian CP-3800 gas chromatograph equipped with three Ni electron capture detectors operated at 370°C . Details of the gas chromatograph setup and operation can be found in Pennock et al.

(2005). The vertical flux was calculated using the diffusion-based model proposed by Hutchinson and Mosier (1981).

A meteorological station was set-up on the SE quarter of section 9. The station measured air temperature, precipitation and soil temperature at five depths.

Upscaling of the chamber data was carried out both in time and space. The temporal integration involved transfer of the fluxes measured in a 30-min observation period to longer time periods. Upscaling spatially to the township level involved multiplying the average total flux measured for a specific crop and fertilizer class by the area of that class resulting in units of $\text{kg N}_2\text{O-N}$.

Cumulative emissions at snowmelt for each site were calculated by extrapolating the flux observed during the measurement period to the total time period between measurements. For example, the flux on CD 95 (i.e., Table 1, in $\text{mg N}_2\text{O-N m}^{-2} \text{ d}^{-1}$) was multiplied by the time interval between noon on CD 94 to noon on CD 97. The duration of the sampling period was 14 days. Hence all total flux measurements have implicit units of 14 days associated with them.

An EW/NS grid flight pattern including six flight tracks was used to quantify N_2O fluxes over the $9.6 \text{ km} \times 9.6 \text{ km}$ experimental cropland site located east of Laird. Measurements were made over approximately 9-km long transects flown back and forth near midday, when the turbulence in the atmospheric surface layer was well developed. Another site, 200 km further North located close to Melfort ($52^{\circ}50'\text{N}$ and $104^{\circ}42'\text{W}$), with slightly higher soil moisture conditions, was also used to characterize the impact of the precipitation gradient on the flux dynamic. Two transect flight patterns were established, a N–S and an E–W track, each about 19 km in length. The REA and EC flux measurements were obtained at approximately 60 m above the ground. Under these relatively stable conditions, the flux footprint contributing to 80% of the flux was estimated to be about 3.6 km (Schuepp et al., 1990). A dead band was set to 0.05 m s^{-1} during the REA sampling.

Air samples collected using the aircraft during the field campaign of Laird in 2002 were analyzed for N_2O concentration differences soon after landing using a TGA100 instrument. The TDL was set up in the gradient mode to measure concentration differences between the Up and the Down bags of individual pairs previously sampled in flight. The flux resolution for this study was estimated to be about $0.27 \text{ mg N}_2\text{O-N m}^{-2} \text{ d}^{-1}$ based on an accuracy of 10 pptv on the N_2O concentration difference and a standard deviation of the gust velocities of 0.5 m s^{-1} .

Table 1

Daily ($\text{mg N}_2\text{O-N m}^{-2} \text{d}^{-1}$) and cumulative ($\text{kg N}_2\text{O-N ha}^{-1}$) N_2O flux values calculated for the Laird (Sask.), 2002 study using chamber-based (Pennock et al., 2005) and aircraft-borne sensors measurements and the DNDC model

	CD						Cumulative
	95	99	101	103	105	107	
Chamber							
Canola	0.98 (0.69)	0.22 (0.37)	1.37 (0.32)	0.31 (0.60)	0.21 (0.50)	-0.26 (0.26)	0.075 ^a
Peas	1.35 (0.47)	0.06 (0.26)	0.83 (0.63)	0.58 (0.17)	0.21 (0.31)	0.25 (0.40)	0.080 ^a
Wheat	1.87 (0.32)	0.10 (0.14)	1.58 (1.05)	0.73 (0.58)	0.08 (0.02)	-0.07 (0.05)	0.106 ^a
Manure	1.31	0.67	10.35	1.64	1.87	-0.30	0.331 ^a
Laird site	1.52 ^b	0.12 ^b	1.45 ^b	0.65 ^b	0.16 ^b	-0.05 ^b	0.093 ^b
DNDC							
Canola	0	0	0	0.82	0.82	0.90	0.051
Peas	0	0	0	0.85	0.80	0.87	0.051
Wheat	0	0	0	0.95	0.92	0.96	0.058
Manure	0	0	0	1.21	1.32	1.14	0.077
Laird site	0 ^b	0 ^b	0 ^b	0.97 ^b	0.95 ^b	0.99 ^b	0.054 ^b
Aircraft	-0.03	0.32	0.11	1.14	0.45	0.26	0.048

Standard deviations of chamber measurements are indicated in parenthesis.

^a Cumulative emissions are the sum of products of the observed emissions on each day times the time period.

^b The cumulative area-integrated emissions for the chambers are the product of the cumulative emission for each crop × the area of the township the crop occupied.

3. Results of snowmelt measurement program

Nitrous oxide emissions are presented for tower-based measurements obtained at an Eastern Canada site in 1997, and for measurements made by chamber and aircraft methods, obtained at a Western Canada site in 2002. In addition, the data from both sites were simulated by the DNDC model and the estimation and measured data compared.

3.1. Tower measurements at the Eastern Canada site of Ottawa

The soil freezing depth reached about 0.40 m during the winter. Three cooling-warming cycles, which kept the upper soil layers frozen, were observed prior the start of the final soil thawing (Fig. 2). The final snowmelt started on day 91, when the snow cover was 0.25 m deep. The snow was gone by day 97. The end of the soil thawing period was about day 110. The flux measurements in early March did not indicate any emissions when the soil warmed up, but was still frozen, following significant rainfall. The series of precipitation events experienced generated slightly negative fluxes. Most of the emissions in the atmosphere were synchronized with the progression of the thawing in the soil profile. A significant portion of N_2O formed in the soil profile over the winter was trapped by the ice layer (Teepe et al., 2001) until it could be released with

thawing. Thawing at 0.10 and 0.20-m depth generated the highest release in the atmosphere. The highest daily emission occurred on day 114 and was about 11 $\text{mg N}_2\text{O-N m}^{-2}$. Deeper soil layers contributed also to significant emissions when they warmed up. Nitrous oxide release to the atmosphere reached a background level of 1 $\text{mg N}_2\text{O-N m}^{-2} \text{d}^{-1}$ around day 127. The cumulative emissions during the spring thaw were 1.26 $\text{kg N}_2\text{O-N ha}^{-1}$.

With temporal integration in mind, a test was run to assess the frequency with which chamber measurements would be required to determine the average obtained with tower-flux measurements. The approach consisted in extracting the 30-min flux data at 11:00 h to simulate discrete chamber sampling for quantifying N_2O flux (Fig. 3a). The following simulated chamber sampling strategies were tested: measuring once a day, twice a week and once a week. A shift in the starting day was also introduced to evaluate the impact on the cumulative estimate for sampling once and twice a week (Fig. 3b). For the sampling strategies illustrated in Fig. 3a, there is a large difference in the cumulative emissions using all the 30-min data in comparison to estimating fluxes once a day (+15%), twice or once a week (+26%). By shifting the starting day (Fig. 3b), the cumulative emissions when sampling once a week ranged from -8 to +27% of the cumulative value obtained from continuous sampling. The range was narrower (12–26%) when simulating sampling twice a

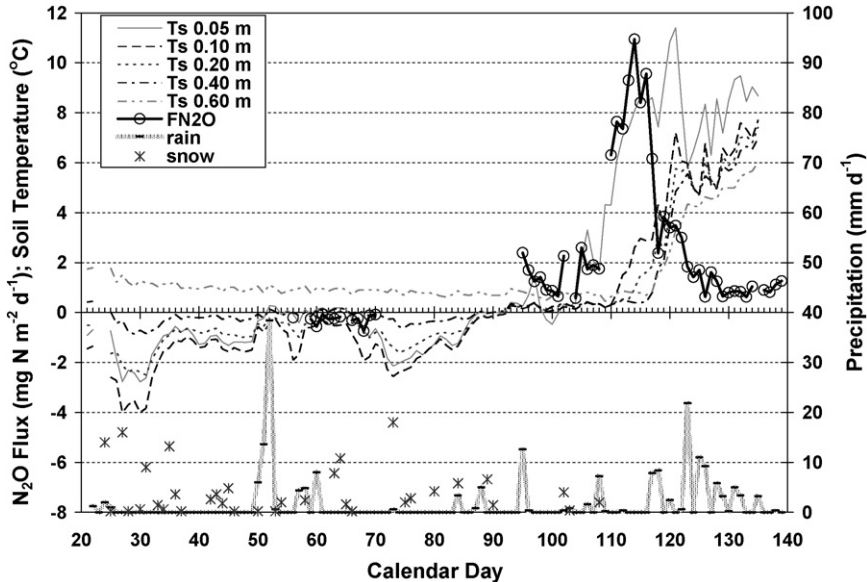


Fig. 2. Spring thaw N₂O emissions from the harvested corn field close to Ottawa (Ont.). Daily soil temperature and precipitation during spring thaw.

week. Sampling twice a week appears to be a minimum for capturing the temporal trend of N₂O emissions associated with spring thaw. Capturing the contribution of N₂O emission fluctuations would require sampling several times per day at evenly spaced intervals. This strategy is not easily achievable with chambers when they cannot be easily automated.

3.2. Chamber measurements at the Western Canada site of Laird

Chamber measurements (Pennock et al., 2005) at the Laird site were carried out over 12 days in 2002. Table 1 and Fig. 4a, which summarize the chamber data for the Laird site for the upscaled data, indicate that the highest emissions occurred on CD 95 for the peas and wheat residues and CD 101 for the manure and canola sites. Emissions decreased on CD 99, increased through CD 101, and then decreased to CD 105, and many sites had negligible emissions or were acting as minor sinks by CD 107. The first peak of emissions on day 95 was not associated with soil thawing of the surface layers (Fig. 4b). According to the observations, soil thawing of the surface soil layer (up to 0.15 m) started on day 117; however, DNDC estimated a first soil thawing during the gap period in soil temperature measurements between CD 101 and 109. This lack of synchronization between chamber emissions and soil thawing suggests that the chambers might have accelerated soil thawing where the measurements were done. The soil was still

frozen at the 0.30-m depth at the end of the observation period.

The cumulative fluxes for each crop type at the Laird site (Table 1) show a clear pattern associated with crop type—the lowest total flux occurs at the canola sites (0.075 kg N₂O-N ha⁻¹), increasing to 0.080 kg N₂O-N ha⁻¹ at the pea sites and 0.106 kg N₂O-N ha⁻¹ at the wheat sites. The highest cumulative emissions were measured over the manure treated site (0.331 kg N₂O-N ha⁻¹).

3.3. Aircraft measurements at Western Canada sites of Laird and Melfort

The aircraft measurements were carried out in 2002 during snowmelt between CD 92 and 109. When the measurement began on day 92, weather was clear and cold, the air temperature was about -13 °C at 60 m above the Laird area. The ground was covered with a shallow snow layer. By the time of the fourth flight on day 99, air temperature had increased to -3 °C, and the soil surface was about 85% snow covered. Two days later (i.e., day 101, fifth flight), air temperature had risen to about 10 °C, and the snow was about 50% gone. There was a gradient in the snow cover, with the northern part of the project area retaining more snow than the southern one (Pennock et al., 2005). At this time, a 6–8 m s⁻¹ wind from the south was advecting warm air over the project area from bare fields to the south. With the cold surface, and warm air aloft, it was

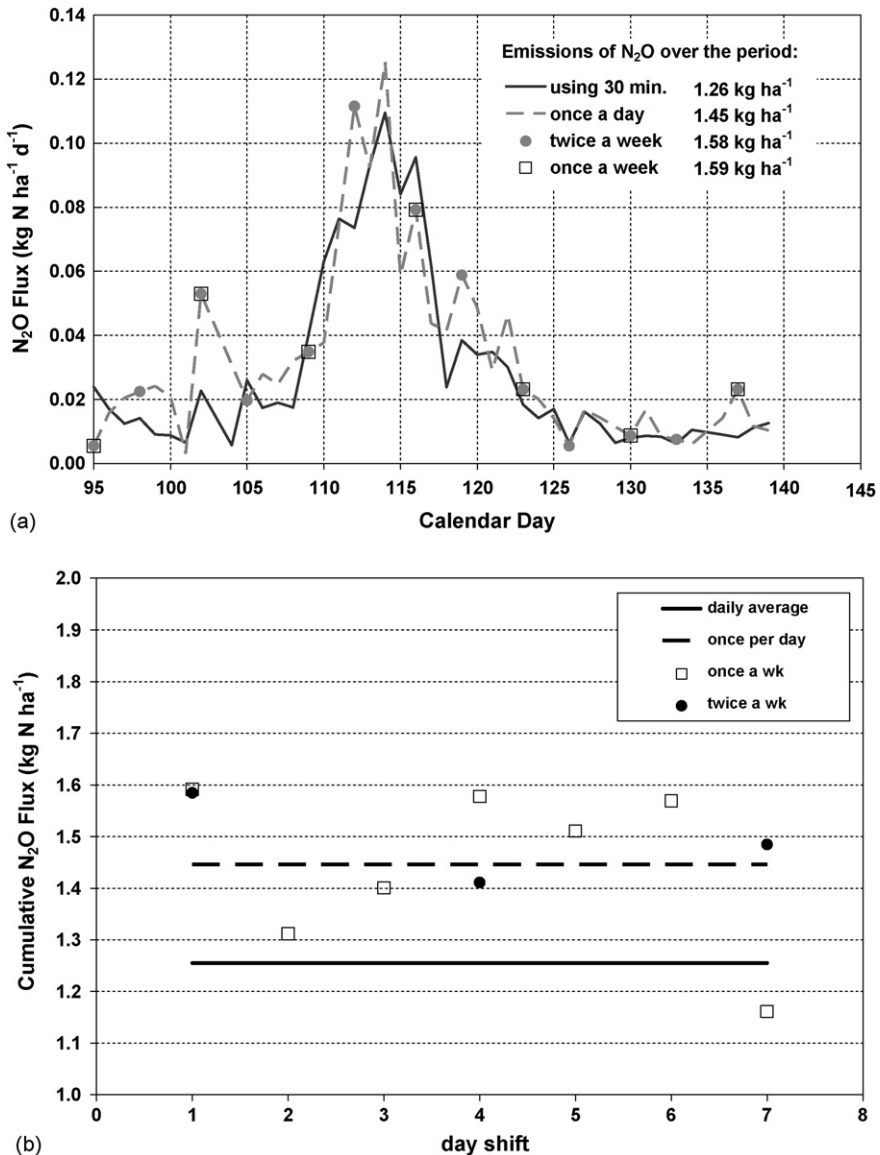


Fig. 3. (a) Simulation of several chamber sampling frequencies using the tower-based N_2O fluxes and their impact on the total emission and (b) variation of the total N_2O emission estimation as a function of the initial starting day of chamber sampling simulations.

very stable with the lowest turbulent gust velocities of the experiment. The sensible heat fluxes measured by the Twin Otter on this day were small and downward. The next day (day 102), air temperature remained near 10°C and only about 5% of the snow cover remained.

Once the snow had all melted in the Laird area, it was decided to broaden the flight program to a second area with slightly higher soil moisture conditions, over which four flights were carried out. The area chosen was southwest of Melfort (Sask.), where the snowmelt was about 2 days later than that of the Laird area.

The average fluxes (Fig. 4a, Table 1) at the Laird site were very low for all flights, about $0.3 \text{ mg N m}^{-2} \text{ d}^{-1}$, which is close to the resolution of the REA system, except flight 7 (day 103), for which it was about $1.1 \text{ mg N m}^{-2} \text{ d}^{-1}$. This was the day with the warmest air and surface temperatures and highest average latent heat flux (112 W m^{-2}) measured at the Laird site. For almost all of the other flights, surface temperatures remained in the $10\text{--}17^\circ\text{C}$ range.

The mean fluxes at Melfort (Sask.) were substantially higher than at Laird, with the largest flux (i.e., $1.44 \text{ mg N m}^{-2} \text{ d}^{-1}$) on CD 105, in conjunction with

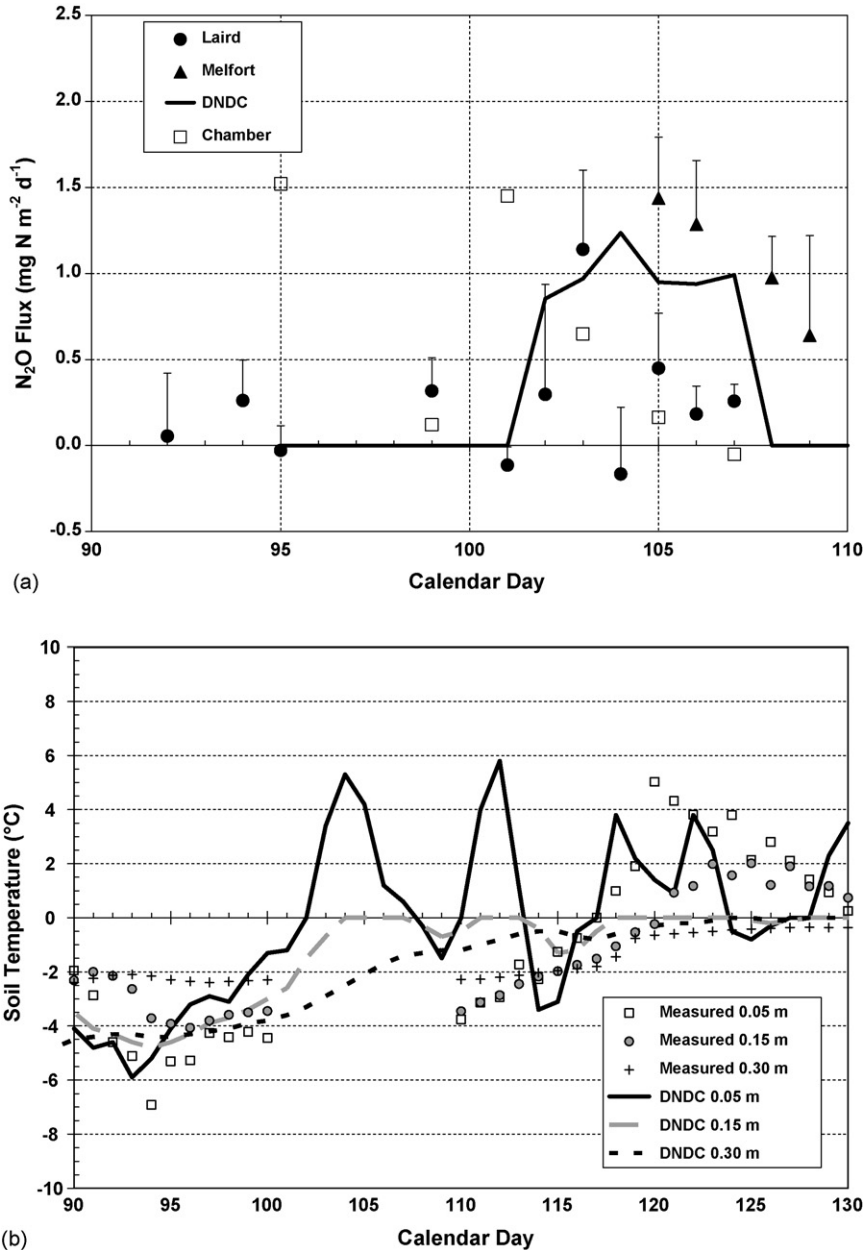


Fig. 4. Comparison of measurements and estimates using DNDC of (a) N_2O fluxes and (b) daily soil temperature for Western, Laird (Sask.) study site. The aircraft measurements in 2002 are shown for both the dryer Laird site (Sask.) and the wetter Melfort site (Sask.). The chamber measured for the Laird site and the DNDC estimates for the same site integrated over the four crop/management cases.

the highest latent heat flux measured in the entire experiment (Fig. 4a). On subsequent flights at Melfort, the flux started to decline, suggesting that the peak occurred on or just before CD 105.

The low N_2O emissions in Western Canada during the spring of 2002 were not entirely unexpected because of the lower amount of fertilizer used in Western Canada and the substantially drier soil conditions than in Eastern Canada. Snow pack north of Saskatoon for

the winter of 2001–2002 was well below average. Snow melted rapidly over about 3 days.

3.4. Aircraft/chamber comparison, Western Canada site at Laird

Cumulative fluxes over the snowmelt period for the chamber-based measurements and the aircraft-based sensors were compared. The experiment offered an

opportunity to evaluate how well the two methods can be used to estimate N_2O fluxes at a regional scale. To complete this comparison, the aircraft-based measurements for the days on which field chamber measurements were also made (i.e., days 95, 99, 101, 103, 105, and 107) were temporally integrated using the same procedure as was used for the chamber-based measurement (Table 1 and Fig. 4).

The overall area-integrated cumulative emissions calculated from the chamber ($0.093 \text{ kg N}_2\text{O-N ha}^{-1}$) were twice as large as the aircraft data ($0.048 \text{ kg N}_2\text{O-N ha}^{-1}$) but both averages are in the same low range. The day-to-day agreement between the chamber crop averages from the 12 sites and the aircraft-based sensors was low. The chamber measurement detected the peak emissions on CD 95, 7 days prior to the aircraft initial peak detection, which coincides with soil thawing. The chamber-based sampling is of 12 fields out of 144 in the township; the actual chambers measure emissions from a total area of approximately 1 m^2 out of each field of approximately $640\,000 \text{ m}^2$. The small area that is actually sampled, coupled with the different temporal patterns of emissions observed at the 12 sites, mean that the likelihood that daily emissions from the chambers will be consistently similar to the whole-township average from the aircraft is very small. As previously mentioned, chambers might have altered the environmental conditions by speeding up soil thawing. Further, this suggests that while chamber method may be useful for making relative assessment of treatment effects, their use for quantifying spatial and temporal effects on N_2O flux is limited.

3.5. Measurement model comparisons, Eastern and Western Canada sites

The DNDC model was used to estimate the experimental results obtained at the Eastern field site where measurements during the spring thaw period were obtained and for the Western, Laird Saskatchewan site. The results are reported below.

3.5.1. Eastern Canada site, Ottawa, Ontario, 1997

Soil properties used in the simulation of the Ottawa field site were, bulk density: 1.25 g cm^{-3} , organic matter: 6.3%, passive fraction (humus): 80%, clay fraction: 0.39, soil texture: clay loam, gravimetric field capacity/wilting point, 0.57/0.27. The simulation period used was 3 years (1995–1997). The crop rotation over this period was barley–corn–corn. Urea fertilization was applied at a rate of 70 kg N ha^{-1} on barley and

138 kg N ha^{-1} on corn. Zero tillage was assumed and the water table was assumed to be at 0.50 m. Climatic inputs consisted of daily minimum and maximum air temperature and precipitation from the Ottawa airport located 5 km east of the site.

In 1997, the cumulative tower-based fluxes measured over an harvested corn field under no-tillage management for CD 95–139 was about $1.26 \text{ kg N}_2\text{O-N ha}^{-1}$. DNDC estimated that during the same period approximately $0.82 \text{ kg N}_2\text{O-N ha}^{-1}$ would be emitted (Fig. 5a).

Under closer examination of the comparison, DNDC was able to capture the initial timing of the spring N_2O emissions fairly well but had some problems in reproducing the flux patterns observed. Timing of the spring burst is regulated by the ability of the DNDC model to simulate the proper soil temperatures and encapsulate any freezing and thawing events occurring during that period. Comparing soil temperatures measured over the same time frame against DNDC estimates for 0.05, 0.15 and 0.30-m depths revealed that the model was able to estimate reasonably well changes in soil temperature for the various depths (Fig. 5b). At the 0.15 and 0.30-m depths there were some variations between measured and estimated results once the snow pack had melted at day 108 with the model predicting higher soil temperatures faster than the measured results indicate. This might explain why the model estimates a larger flux for day 109 ($8.43 \text{ mg N}_2\text{O-N m}^{-2} \text{ d}^{-1}$) than the measurements indicate ($1.46 \text{ mg N}_2\text{O-N m}^{-2} \text{ d}^{-1}$). The DNDC model also assumes that when there is a snow pack the soil will benefit from an insulating effect. This may explain why soil temperature is different between the measurements and the model estimates before day 108 at the various depths.

Another discrepancy between modeled and measured N_2O emissions occurs on day 131. DNDC estimates that there should be another burst occurring for the next few days. Investigation of the climate data shows that over CD 128–132, the soil received approximately 17.6 mm of rain (Fig. 2). This rainfall addition coupled with the elevated soil moisture and water table was able to drive N_2O production as a result of denitrification in the model (Fig. 5a). This suggests that the field did not reach the same denitrification rates that the model predicted, possibly as a result of low substrate level, as a consequence of nitrate leaching during snowmelt and subsequent precipitation.

3.5.2. Western Canada site, Laird, Saskatchewan, 2002

The DNDC model was used to estimate N_2O emissions from wheat, wheat with manure, canola, and

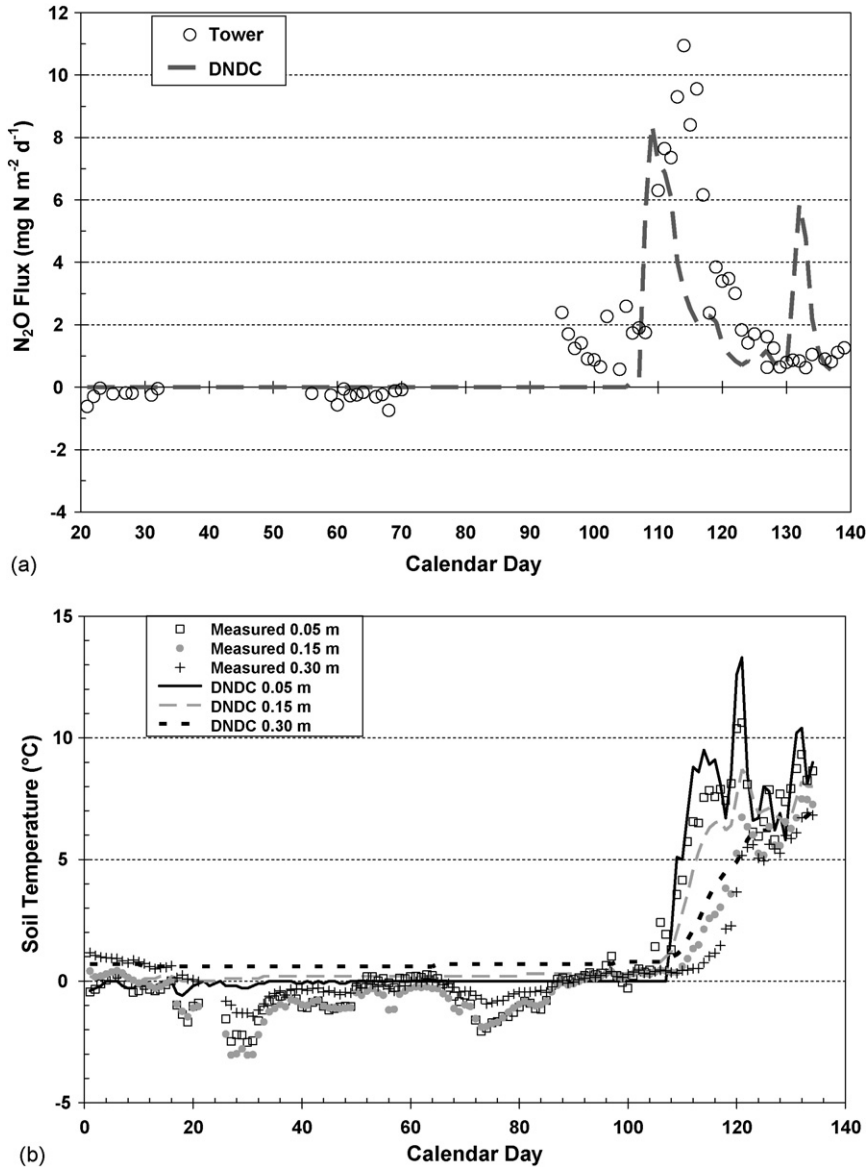


Fig. 5. Comparison of DNDC estimates to measurements: (a) of N_2O fluxes and (b) of soil temperature (T_s) during spring thaw at the Ottawa site (Ont.).

peas. Soil properties and fertilizer application rates were taken from Pennock et al. (2005). On the wheat, 80 kg N ha^{-1} fertilizer was applied, 70 kg N ha^{-1} on canola, and 10 kg N ha^{-1} as a starter on peas. The manure produced from a 30 cow beef farm was spread over two 6.4 ha plots (NW2) four times during the year, 1 February, 1 May, 1 August, and 1 December. The manure characteristics were based on the Manure Management Systems Series from Midwest Plan Service (Lorimor et al., 2000). On each of the four applications 1 t of C was applied at a C:N ratio of 25 and over the year the application rate was estimated to be 160 kg N ha^{-1} .

Actual weather data from the site was used as input to DNDC between CD 86 and 108, otherwise weather data were taken from a station near Laird. The model was run 7 years prior to 2002, the year of interest, to stabilize C and N pools.

Results from each simulated crop and soil were scaled up for the whole test area based on crop area coverage percentages (Pennock et al., 2005). Table 1 presents the results of the comparison of the cumulative emissions from the four crop categories. Table 1 and Fig. 4a show the results of the daily flux comparison. As with aircraft and chamber the daily values of the

chamber and DNDC model did not compare well. The estimated peak emission using DNDC was shifted in relation to the peak emission observed using the chambers (Fig. 4a), while the observed peak emission by the aircraft corresponded reasonably well with the emissions pattern predicted with DNDC and were similar in magnitude (i.e., 1.14 and 1.24 mg N₂O-N m⁻² d⁻¹, respectively).

For the cumulative emissions, the DNDC model and chamber measurements compared quite well. The DNDC model underestimated emission from the manure treatment. However, manure application only occurred on 1.3% of the test area. The DNDC underestimation may partly be because the model underestimated soil temperatures and decomposition through enhanced microbial activity at the 0.15 and 0.30-m depths. On average the estimated emissions from crops, on which inorganic fertilizer was applied, was slightly lower than the measured values with 0.053 kg N₂O-N ha⁻¹ from DNDC versus 0.087 kg N₂O-N ha⁻¹ from chamber measurements. Using known percentages of field crops at the site, emission estimates were scaled up for the entire study region and compared to emissions from the chamber and aircraft transect studies. The DNDC model predicted emissions of 0.054 kg N₂O-N ha⁻¹ over the study period which was between the aircraft measurements of 0.048 kg N₂O-N ha⁻¹ and the chamber measurements of 0.094 kg N₂O-N ha⁻¹.

4. Discussion and conclusions

Intercomparison of data from various tools has led to insightful understanding of N₂O emission. Although the chamber flux, integrated over the entire snowmelt period and for several crop categories predicted average flux in the same range as the aircraft measurements at a Western Canada site, the day-to-day comparison was poor. Nitrous oxide emissions measured using the aircraft were well synchronized with soil thawing, while the chambers seemed to have altered the soil energy balance and accelerated the soil thawing by a couple of days.

Tower-based measurements provided a high resolution time series of emissions during the snowmelt period, with some undersampling of nighttime emissions. They fill a gap during a significant emission period when chamber measurements would be challenging to carry out and would cause a lot of disturbance to the soil environment. For the dataset available, the simulations of chamber sampling strategies showed clearly that the coarser time resolution led to an overestimation during the spring thaw period. However,

this trend cannot be extrapolated to other sampling periods.

Comparison of the tower-based and aircraft flux measurements during snowmelt gave good agreement with the DNDC model, when thawing occurred rapidly. The DNDC model predicted the overall snowmelt emission within a few percent of the aircraft estimates. The timing of emissions between DNDC and the tower measurements was well synchronized. Similar low numbers were produced between the DNDC model and the chamber for each crop type.

Although the temporal comparison is limited, considerable divergence in emissions from snowmelt was observed between Western and Eastern Canada, which is most likely due to climatic and fertilizer use differences. Fluxes measured at the Western Canada site were substantially lower than at the Eastern Canada site. This trend has been reported in the literature. Table 2 summarizes current literature for Western and Eastern Canadian sites. It is important to note, however, that emissions from Eastern Canada show very high annual variability. Van Bochove et al. (2000, 2001) detected order-of-magnitude differences between years, attributed primarily to differences in the soil moisture conditions in the preceding year and to the timing and depth of the snow pack.

The emissions observed in the 2002 snowmelt event at Laird (Sask.) are at the low end of the range of snowmelt emissions observed for cropland in Western Canada. The range of maximum daily flux for non-manured cropped sites at Laird is comparable to the lower emissions range of Corre et al. (1999) and Lemke et al. (1998) but are well below the higher maximum emissions of Lemke and all of the Nyborg et al. (1997) calculated rates.

The results of Pennock and Corre (2001), from Hepburn (Sask.), are from a spring thaw following a year with above-average precipitation. The maximum emissions from midslope position in their study using chambers are about three times higher than the non-manured cropland maximum rates from the 2002 Laird study. Emissions from depressions in spring, 1997 were also higher than the Laird 2002 results. Water filled pore space for the midslopes in the Hepburn study ranged from 60 to 80% (i.e., the optimum range for N₂O emissions), and the depressions were between 72 and 100%. Pennock and Corre (2001) suggest that the lower emissions from depressions were due to enhanced production of N₂ at the expense of N₂O.

Comparisons of total emissions associated with the snowmelt period are more difficult because of the differences in measurement methods and the upscaling

Table 2

N₂O emissions during spring thaw from field studies in Western and Eastern Canada

Author and location	Treatment, year, position	Maximum N ₂ O emission (mg N ₂ O-N m ⁻² d ⁻¹)	Cumulative N ₂ O flux (kg N ₂ O-N ha ⁻¹)
Corre et al. (1999), St. Louis, Sask.	Sandy forest convex position	0.025 ^a	
	Sandy forest concave position	0.020	0.003
	Sandy pasture convex position	0.020	
	Sandy pasture concave position	0.350	0.027
	Sandy oats convex position	0.289	
	Sandy oats concave position	0.999	0.120
	Fine sandy loam, canola residue, convex position	1.500	
	Fine sandy loam, canola residue, concave position	1.151	0.047
	Clay loam pasture, 1994	0.100	
	Clay loam forest, 1994	0.199	0.038
	Clay loam pasture, 1995	0.070	
	Clay loam forest, 1995	0.300	0.036
	Clay loam canola, convex position	1.500	
	Clay loam canola, concave position	2.000	0.200
Grant and Pattey (1999), Ottawa, Ont.	Harvested barley field, 1996	16.776	1.36
Lemke et al. (1998, 1999), Ellerslie, Alta.	Intensive tillage, fertilizer treatment, 1993	4.1 ^a	0.54
	Intensive tillage, fertilizer treatment, 1994	1.679	0.15
	Intensive tillage, fertilizer treatment, 1995	31.200	1.81
	Zero tillage, fertilizer treatment, 1993	2.879	0.28
	Zero tillage, fertilizer treatment, 1994	1.139	0.23
	Zero tillage, fertilizer treatment, 1995	4.800	0.40
Lemke et al. (1998, 1999), Breton, Alta.	Intensive tillage, fertilizer treatment, 1993	3.360	0.15
	Intensive tillage, fertilizer treatment, 1994	0.600	0.05
	Intensive tillage, fertilizer treatment, 1995	2.159	0.23
	Zero tillage, fertilizer treatment, 1993	0.959	0.06
	Zero tillage, fertilizer treatment, 1994	0.419	0.04
	Zero tillage, fertilizer treatment, 1995	2.040	0.19
Nybørg et al. (1997), Ellerslie Alta.	Added fall N, 1989	11.100	1.30
	No added fall N, 1989	40.599	3.50
	Added fall N, 1990	68.299	6.00
	No added fall N, 1990	209.298	16.30
Pennock and Corre (2001), Hepburn Sask.	Midslope, 0 kg ha ⁻¹ N added	5.499	0.34
	Midslope, 42 kg ha ⁻¹ N added	3.499	0.28
	Midslope, 84 kg ha ⁻¹ N added	1.750	0.12
	Midslope, 126 kg ha ⁻¹ N added	7.799	0.53
	Midslope, 168 kg ha ⁻¹ N added	6.100	0.45
	Depression, 0 kg ha ⁻¹ N added	0.999	0.09
	Depression, 42 kg ha ⁻¹ N added	5.000	0.09
	Depression, 84 kg ha ⁻¹ N added	1.899	0.15
	Depression, 126 kg ha ⁻¹ N added	2.100	0.11
	Depression, 168 kg ha ⁻¹ N added	8.999	0.32
Van Bochove et al. (2000), Levis, Que.	1994–1995, barley, February	3.410 ^b	
	February–March	2.419	
	Initial melt, March–April	8.031	
	Main melt, April	3.244	4.40
	1995–1996, barley, February	0.439	
	February–March	0.219	
	Initial melt, March–April	0.436	
	Main melt, April	No measurable flux	0.40

Table 2 (Continued)

Author and location	Treatment, year, position	Maximum N ₂ O emission (mg N ₂ O-N m ⁻² d ⁻¹)	Cumulative N ₂ O flux (kg N ₂ O-N ha ⁻¹)
Wagner-Riddle et al. (1997), Elora, Ont.	1993–1994, fallow	2.96	
	Manured fallow	2.69	
	Alfalfa	0.10	
	Grass	-0.10	
	1994–1995, fallow	2.64	
	Manure–Fallow	4.34	
	Alfalfa	2.46	
	Grass	0.09	
	Corn	1.46	
Maggiotto and Wagner-Riddle (2001), Elora, Ont.	1997–1998, rye grass, three different fertilizer regimes	7.085	
Burton and Beauchamp (1994), Delhi, Ont.	1988–1989	24.883	
	1989–1990	29.894	
Pennock et al. (2005), Laird, Sask.	NW2, manure, barley residue	7.999	0.162
	SW4, wheat	2.143	0.055
	SW6, pea	1.207	0.045
	NE13, wheat	1.359	0.042
	SE13, canola	1.382	0.021
	SW13, wheat	1.526	0.035
	SE21, pea	1.963	0.043
	SW21, canola	0.714	0.005
	SE22, canola	1.200	0.040
	SW22, canola	0.641	0.014
	NE27, peas	0.936	0.024
	SE34, peas	0.924	0.026

Values shown are the maximum N₂O flux observed during the sampling period (in mg N₂O-N m⁻² d⁻¹) and the cumulative N₂O flux (kg N₂O-N ha⁻¹) over the measurement period.

^a Interpolated from graphs.

^b Flux observed on sampling day may not represent maximum flux for period.

methods used specifically in the period over which the measurements are extrapolated. For example the cumulative emissions calculated for non-manured cropland sites at Laird are all below 0.11 kg N₂O-N ha⁻¹; even the manured site has cumulative emissions of 0.33 kg N₂O-N ha⁻¹. These are in the same range as the cumulative emissions from St. Louis, Saskatchewan, sites in Corre et al. (1999), and the two lowest cumulative values from Lemke et al. (1998) (i.e., snowmelt in 1994 at Breton). They represent a small fraction of the Nyborg et al. (1997) values, but these cumulative emissions were calculated using a very different upscaling approach and cannot be readily compared to our study.

In conclusion, N₂O quantification cannot be assessed with a single tool because the emissions are sporadic both in time and space. However, we now have the tools to verify model estimates over space and time and in relation to ambient conditions. More N₂O flux measurements in conjunction with ancillary descriptors

should be carried out using tower and aircraft to verify process-based models and derive a set of controlling factors relevant to the mapping of emissions from individual fields at the regional scale. This kind of data is essential to reduce the uncertainty associated with the national inventories of N₂O emissions.

Acknowledgements

We gratefully acknowledge the assistance of Chuck Taylor and the crew from the Flight Research Laboratory of NRC for assisting with the data collection on the aircraft, Dave Dow and Richard Riznek during the field campaign in Saskatchewan, Dave Dow and Mark Edwards for the tower-based flux measurements. The research was conducted with the support of CCFIA and Agriculture and Agri-Food Canada's PERD program. We thank Drs Con Campbell and Christian de Kimpe for their helpful comments. ECORC contribution #05-510.

References

- Bouwman, A.F., 1990. Exchange of greenhouse gases between terrestrial ecosystems and the atmosphere. In: Bouwman, A.F. (Ed.), *Soils and the Greenhouse Effect*. John Wiley, Chichester, pp. 61–127.
- Burton, D.L., Beauchamp, E.G., 1994. Profile nitrous oxide and carbon dioxide concentrations in a soil subject to freezing. *Soil Sci. Soc. Am. J.* 58, 115–122.
- Businger, J.A., Oncley, S.P., 1990. Flux measurement with conditional sampling. *J. Atmos. Ocean. Technol.* 7, 349–352.
- Cates, R.L., Keeney, D.R., 1987. Nitrous oxide production throughout the year from fertilized and manured maize fields. *J. Environ. Qual.* 16, 443–447.
- Corre, M.D., Pennock, D.J., van Kessel, C., Elliot, D.K., 1999. Estimation of annual nitrous oxide emissions from transitional grassland-forest region in Saskatchewan, Canada. *Biogeochemistry* 44, 29–49.
- Desjardins, R.L., 2004. The impact of management strategies in agriculture and agroforestry to mitigate greenhouse gas emissions. In: *Management Strategies in Agriculture, Forestry for Mitigation of Greenhouse Gas Emissions, Adaptation to Climate Variability, Climate Change*. WMO No. 969. Technical Note No. 202, pp. 30–40.
- Desjardins, R.L., MacPherson, J.I., Schuepp, P.H., 2000. Aircraft-based flux sampling strategies. In: Meyers, R.A. (Ed.), *Encyclopedia of Analytical Chemistry*. John Wiley & Sons Ltd., Chichester, pp. 3573–3588.
- Dörsch, P., Palojärvi, A., Mommertz, S., 2004. Overwinter greenhouse gas fluxes in two contrasting agricultural habitats. *Nutr. Cycl. Agroecosyst.* 70, 117–133.
- Edwards, G.C., Dias, G.M., Thurtell, G.W., Kidd, G.E., Roulet, N.T., Kelly, C.A., Rudd, J.W.M., Moore, A., Halfpenny-Mitchell, L., 2001. Methane flux from a wetland using the flux gradient technique. *Water Air Soil Pollut. Focus* 1, 447–454.
- Edwards, G.C., Neumann, H.H., den Hartog, G., Thurtell, G.W., Kidd, G., 1994. Eddy correlation measurements of methane fluxes using a tunable diode laser at the Kinosheo Lake tower site during the Northern Wetlands Study (NOWES). *J. Geophys. Res.* 99, 1511–1517.
- Edwards, G.C., Thurtell, G.W., Kidd, G.E., Dias, G.M., Wagner-Riddle, C., 2003. A diode laser based gas monitor suitable for measurement of trace gas exchange using micrometeorological techniques. *Agric. For. Meteorol.* 115, 71–89.
- EPA, 2001. Inventory of US Greenhouse Gas Emissions and Sinks: 1990–1999. EPA.
- Gash, J.H.C., 1986. A note on estimating the effect of a limited fetch on micrometeorological evaporation measurements. *Bound. Layer Meteorol.* 35, 409–413.
- Goodroad, L.L., Keeney, D.R., 1984. Nitrous oxide emissions from soils during thawing. *Can. J. Soil Sci.* 64, 187–194.
- Grant, B., Smith, W., Desjardins, R.L., Lemke, R., Li, C., 2004. Estimated N_2O and CO_2 emissions as influenced by agricultural practices in Canada. *Clim. Change* 65, 315–332.
- Grant, R.F., Pattey, E., 1999. Mathematical modelling of nitrous oxide emissions from an agricultural field during spring thaw. *Global Biogeochem. Cycl.* 13 (2), 679–694.
- Grant, R.F., Pattey, E., 2003. Modelling variability in N_2O emissions from fertilized agricultural fields. *Soil Biol. Biochem.* 35 (2), 225–243.
- Hicks, B.B., 1976. Wind profile relationships from the Wangara experiment. *Quart. J. R. Meteorol. Soc.* 102, 535–551.
- Hutchinson, G.L., Mosier, A.R., 1981. Improved soil cover method for field measurement of nitrous oxide fluxes. *Soil Sci. Soc. Am. J.* 45, 311–316.
- IPCC (International Panel on Climate Change), 1997. Greenhouse gas emissions from Agricultural soils. In: Houghton, J.T., et al. (Eds.), *Greenhouse Gas Reference Manual Revised 1996*. IPCC Guidelines for National Greenhouse Gas Inventories, vol. 3, Sec. 4.5. Agriculture IPCC/OECD/IEA. UK Meteorological Office, Bracknell, UK.
- Kaiser, E.A., Kohrs, K., Kücke, M., Schnug, E., Heinemeyer, O., Munch, J.C., 1998. Nitrous oxide release from arable soil: importance of N-fertilization, crops and temporal variation. *Soil Biol. Biochem.* 30, 1553–1563.
- Laville, P., Jambert, C., Cellier, P., Delmas, R., 1999. Nitrous oxide Fluxes from a fertilised maize crop using micrometeorological and chamber methods. *Agric. For. Meteorol.* 96, 19–38.
- Lemke, R.L., Izaurrealde, R.C., Nyborg, M., 1998. Seasonal distribution of nitrous oxide emissions from soils in the Parkland region. *Soil Sci. Soc. Am. J.* 62, 1320–1326.
- Lemke, R.L., Izaurrealde, R.C., Nyborg, M., Solberg, E.D., 1999. Tillage and N source influence soil-emitted nitrous oxide in the Alberta Parkland region. *Can. J. Soil Sci.* 79, 15–24.
- Li, C., Frolking, S., Frolking, T.A., 1992a. A model of nitrous oxide evolution from soil driven by rainfall events. I. Model structure and sensitivity. *J. Geophys. Res.* 97, 9759–9776.
- Li, C.S., Frolking, S., Frolking, T.A., 1992b. A model of nitrous oxide evolution driven by rainfall events. II. Model applications. *J. Geophys. Res.* 97, 9777–9783.
- Li, C.S., Frolking, S., Harris, R., 1994. Modeling carbon biogeochemistry in agricultural soils. *Global Biogeochem. Cycl.* 8, 237–254.
- Li, C., Aber, J., 2000. A process-oriented model of N_2O and NO emissions from forest soils. I. Model development. *J. Geophys. Res.* 105, 4369–4384.
- Livingston, G.P., Hutchinson, G.L., 1995. Enclosure-based measurement of trace gas exchange: applications and sources of error. In: Matson, P.A., Harriss, R.C. (Eds.), *Biogenic Trace Gases: Measuring Emissions from Soil and Water*. Blackwell Science Ltd., Oxford, UK, pp. 14–51.
- Lorimor, J., Powers, W., Sutton, A., 2000. Manure Characteristics. MWPS-18 Manure Management Systems Series. Midwest Plan Service, Ames, IA.
- MacPherson, J.I., Desjardins, R.L., 1991. Airborne tests of flux measurement by the relaxed eddy accumulation technique. In: *Proceedings of the Seventh AMS Symposium on Meteorological Observations and Instrumentation*, New Orleans, LA, January 14–18, 1991, pp. 6–11.
- MacPherson, J.I., Marcotte, D.L., Jordan, J.E., 2001. The NRC atmospheric research aircraft. *Can. Aeron. Space Inst.* 47, 147–157.
- Maggiotto, S.R., Wagner-Riddle, C., 2001. Winter and spring thaw measurements of N_2O , NO and NO_x fluxes using a micrometeorological method. *Water Air Soil Pollut. Focus* 1, 89–98.
- Mosier, A.R., Duxbury, J.M., Freney, J.R., Heinemeyer, O., Minami, K., 1994. Nitrous oxide emissions from agricultural fields: assessment, measurement and mitigation. In: *Proceedings of the Nitrogen Workshop*, Gent, Belgium.
- Nyborg, M., Laidlaw, J.W., Solberg, E.D., Mahli, S.S., 1997. Denitrification and nitrous oxide emissions from a Black Chernozemic soil during spring thaw in Alberta. *Can. J. Soil Sci.* 77, 153–160.
- Parton, W.J., Holland, E.A., Del Grosso, S.J., Hartman, M.D., Martin, R.E., Mosier, A.R., Ojima, D.S., Schimel, D.S., 2001. Generalized for NO_x and N_2O emission from solid. *J. Geophys. Res.* 106, 17403–17419.

- Parton, W.J., Mosier, A.R., Ojima, D.S., Valentine, D.W., Schimel, D.S., Weir, K., Kulmala, K., 1996. Generalised model for N₂ and N₂O production from nitrification and denitrification. *Global Biogeochem. Cycl.* 10, 401–412.
- Pattey, E., Desjardins, R.L., Rochette, P., 1993. Accuracy of the relaxed eddy-accumulation technique evaluated using CO₂ flux measurements. *Bound. Layer Meteorol.* 66, 341–355.
- Pattey, E., Edwards, G., Strachan, I.B., Desjardins, R.L., Kaharabata, S., Wagner-Riddle, C., 2006a. Towards standards for measuring greenhouse gas flux from agricultural fields using instrumented towers. *Can. J. Soil Sci.* 86, 373–400.
- Pattey, E., Strachan, I.B., Desjardins, R.L., Edwards, G.C., Dow, D., MacPherson, I.J., 2006b. Application of a tunable diode laser to the measurement of CH₄ and N₂O fluxes from field to landscape scale using several micrometeorological techniques. *Agric. For. Meteorol.* 136, 222–236 (special issue “Tribute to Marv Wesely”).
- Pattey, E., Strachan, I.B., Desjardins, R.L., Massheder, J., 2002. Measuring nighttime CO₂ flux over terrestrial ecosystems using eddy covariance and nocturnal boundary layer methods. *Agric. For. Meteorol.* 113 (1–4), 145–153.
- Paulson, C.A., 1970. The mathematical representation of wind speed and temperature profiles in the unstable atmospheric surface layer. *J. Appl. Meteorol.* 9, 857–861.
- Pennock, D.J., Corre, M.D., 2001. Development and application of landform segmentation procedures. *Soil Till. Res.* 58, 151–162.
- Pennock, D.J., Farrell, R., Desjardins, R.L., Pattey, E., MacPherson, I.J., 2005. Upscaling chamber-based measurements of N₂O emissions at snowmelt. *Can. J. Soil Sci.* 85 (1), 113–125.
- Potter, C.S., Matson, P.A., Vitousek, P.M., Davidson, E.A., 1996. Process modelling of controls on nitrogen trace gas emissions from soils worldwide. *J. Geophys. Res.* 101, 1361–1377.
- Rochette, P., McGinn, S.M., 2004. Methods for measuring soil-surface gas fluxes. In: Alvarez-Benedí, J., Muñoz-Carpena, R. (Eds.), *Soil–Water–Solute Processes: An Integrated Approach*. CRC Press, Boca Raton, FL, p. 816.
- Schuepp, H.P., Leclerc, M.Y., MacPherson, J.I., Desjardins, R.L., 1990. Footprint prediction of scalar fluxes from analytical solutions of the diffusion equation. *Bound. Layer Meteorol.* 50, 355–373.
- Simpson, I.J., Edwards, G.C., Thurtell, G.W., den Hartog, G., Neumann, H.H., Staebler, R.M., 1997. Micrometeorological measurements of methane and nitrous oxide exchange above a boreal aspen forest. *J. Geophys. Res.* 102, 29331–29341.
- Simpson, I.J., Thurtell, G.W., Kidd, G.E., Lin, M., Demetriades-Shah, T.H., Flitcroft, I.D., Kanemasu, E.T., Nie, D., Bronson, K.F., Neue, H.U., 1995. Tunable diode laser measurements of methane fluxes from an irrigated rice paddy field in the Philippines. *J. Geophys. Res.* 100, 7283–7290.
- Smith, W.N., Desjardins, R.L., Grant, B., Li, C.S., Lemke, R.L., Rochette, P., Corre, M.D., Pennock, D., 2002. Testing the DNDC model using N₂O emissions at two experimental sites in Canada. *Can. J. Soil Sci.* 82, 365–374.
- Smith, W.N., Grant, B., Desjardins, R.L., Lemke, R., Li, C.S., 2004. Estimates of the interannual variations of N₂O emissions from agricultural soils in Canada. *Nutr. Cycl. Agroecosyst.* 68, 37–45.
- Teepe, R., Brumme, R., Beese, F., 2000. Nitrous oxide emissions from frozen soils under agricultural, fallow and forest land. *Soil Biol. Biochem.* 32, 1807–1810.
- Teepe, R., Brumme, R., Beese, F., 2001. Nitrous oxide emissions from soil during freezing and thawing periods. *Soil Biol. Biochem.* 33, 1269–1275.
- UNFCCC (United Nations Framework Convention on Climate Change) Secretariat, 2003. National communications from Parties included in Annex I to the Convention, National greenhouse gas inventory data from Annex I parties for 1990 to 2001. FCCC/WEB/2003/3, 80 pp.
- UNFCCC (United Nations Framework Convention on Climate Change), 2004. Information on national greenhouse gas inventory data from Parties included in Annex I to the Convention for the period 1990–2002, including the status reporting. Executive summary. Conference of the Parties, 10th session Buenos Aires December 6–17, 2004. FCCC/CP/2004/5, 19 pp.
- Van Bochove, E., Jones, H.G., Bertrand, N., Prevost, D., 2000. Winter fluxes of greenhouse gases from snow covered agricultural soil. Intra-annual and international variations. *Global Biogeochem. Cycl.* 14, 113–125.
- Van Bochove, E., Theriault, G., Rochette, P., Jones, H.G., Pomeroy, J.W., 2001. Thick ice layers in snow and frozen soil affecting gas emissions from agricultural soils during winter. *J. Geophys. Res.* 106, 23061–23071.
- Wagner-Riddle, C., Thurtell, G.W., 1998. Nitrous oxide emissions from agricultural fields during winter and spring thaw as affected by management practices. *Nutr. Cycl. Agroecosyst.* 52, 151–163.
- Wagner-Riddle, C., Thurtell, G.W., Kidd, G.K., Beauchamp, E.G., Sweetman, R., 1997. Estimates of nitrous oxide emissions from agricultural fields over 28 months. *Can. J. Soil Sci.* 77, 135.
- Wagner-Riddle, C., Thurtell, G.W., Kidd, G.E., Edwards, G.C., Simpson, I.J., 1996a. Micrometeorological measurements of trace gas fluxes from agricultural and natural ecosystems. *Infrared Phys. Technol.* 37, 51–58.
- Wagner-Riddle, C., Thurtell, G.W., King, K.M., Kidd, G.E., Beauchamp, E.G., 1996b. Nitrous oxide and carbon dioxide fluxes from a bare soil using a micrometeorological approach. *J. Environ. Qual.* 25, 898–907.
- Webb, E.K., Pearman, G.I., Leuning, R., 1980. Correction of flux measurements for density effects due to heat and water vapour transfer. *Quart. J. R. Meteorol. Soc.* 106, 85–100.
- Weinhold, F.G., Frahm, H., Harris, G.W., 1994. Measurements of N₂O fluxes from fertilized grassland using a fast response tunable diode laser spectrometer. *J. Geophys. Res.* 99 (D8), 16537–16567.
- Zahniser, M.S., Nelson, D.D., McManus, J.B., Kebabian, P.L., 1995. Measurement of trace gas fluxes using tunable diode laser spectroscopy. *Phil. Trans. R. Soc. London A* 351, 371–382.
- Zhu, T., Wang, D., Desjardins, R.L., MacPherson, J.I., 1999. Aircraft-based volatile organic compounds flux measurements with relaxed eddy accumulation. *Atmos. Environ.* 33 (12), 1969–1979.